Research Article | Vol. 26, No. 10 | 14 May 2018 | OPTICS EXPRESS 12432
Optics EXPRESS

Experimental characterization of the radio over fiber aided twin-antenna spatial modulation downlink

YICHUAN LI,[1] QIANMEI YANG,[2] IBRAHIM A. HEMADEH,[1] MOHAMMED EL-HAJJAR,[1] CHUN-KIT CHAN,[2] AND LAJOS HANZO[1,*]

[1]*Department of Electronics and Computer Science, University of Southampton, Southampton SO17 1BJ, UK*
[2]*Department of Information Engineering, The Chinese University of Hong Kong, Shatin, Hong Kong, China*
[*]*lh@ecs.soton.ac.uk*

Abstract: In this paper, we present the design and the experimental demonstration of a radio over fiber (RoF) network relying on state-of-the-art spatial modulation (SM), that activates one out of multiple antennas. We propose a novel RoF-aided SM encoding scheme, where the optical single side-band signal generated by a Mach-Zehnder modulator (MZM) is used for both the antenna selection and for the classic modulated symbol selection. The SM encoding is optically processed in a centralized fashion, aiming for the reduction of power consumption and for enabling cost-effective maintenance and management, which can be employed in the context of a cloud radio access network (C-RAN) and a small-cell front-haul. Furthermore, an experimental demonstration of the proposed system is discussed and analyzed, where a 20 km standard single mode fiber (SSMF) is used for transmission. In this experiment, a 2 Gbps transmission relying on two transmit and two receive antennas is achieved with less than 1 dB SNR degradation compared to those operating without RoF.

OCIS codes: (060.0060) Fiber optics and optical communications; (060.1155) All-optical networks.

References and links

1. A. Goldsmith, *Wireless communications* (Cambridge University, 2005).
2. Y. Li, M. El-Hajjar, and L. Hanzo, "Joint space-time block-coding and beamforming for the multiuser radio over plastic fiber downlink," IEEE Transactions on Veh. Technol. **67**, 2781–2786 (2018).
3. D. Novak and R. Waterhouse, "Advanced radio over fiber network technologies," Opt. express **21**, 23001–23006 (2013).
4. A. Checko, H. L. Christiansen, Y. Yan, L. Scolari, G. Kardaras, M. S. Berger, and L. Dittmann, "Cloud RAN for mobile networks—a technology overview," IEEE Commun. Surv. Tutorials **17**, 405–426 (2015).
5. V. Thomas, M. El-Hajjar, and L. Hanzo, "Performance improvement and cost reduction techniques for radio over fiber communications," IEEE Commun. Surv. Tutorials **17**, 627–670 (2015).
6. H. Yang, Y. He, J. Zhang, Y. Ji, W. Bai, and Y. Lee, "Performance evaluation of multi-stratum resources optimization with network functions virtualization for cloud-based radio over optical fiber networks," Opt. express **24**, 8666–8678 (2016).
7. C. X. Wang, F. Haider, X. Gao, X. H. You, Y. Yang, D. Yuan, H. M. Aggoune, H. Haas, S. Fletcher, and E. Hepsaydir, "Cellular architecture and key technologies for 5G wireless communication networks," IEEE Commun. Mag. **52**, 122–130 (2014).
8. E. Basar, M. Wen, R. Mesleh, M. Di Renzo, Y. Xiao, and H. Haas, "Index modulation techniques for next-generation wireless networks," IEEE Access **5**, 16693–16746 (2017).
9. R. Y. Mesleh, H. Haas, S. Sinanovic, C. W. Ahn, and S. Yun, "Spatial modulation," IEEE Transactions on Veh. Technol. **57**, 2228–2241 (2008).
10. I. A. Hemadeh, M. El-Hajjar, S. Won, and L. Hanzo, "Multi-set space-time shift-keying with reduced detection complexity," IEEE Access **4**, 4234–4246 (2016).
11. M. D. Renzo, H. Haas, A. Ghrayeb, S. Sugiura, and L. Hanzo, "Spatial modulation for generalized mimo: Challenges, opportunities, and implementation," Proc. IEEE **102**, 56–103 (2014).
12. G. Smith, D. Novak, and Z. Ahmed, "Technique for optical SSB generation to overcome dispersion penalties in fibre-radio systems," Electron. Lett. **33**, 74–75 (1997).
13. M. Xue, S. Pan, and Y. Zhao, "Optical single-sideband modulation based on a dual-drive MZM and a 120 hybrid coupler," J. Light. Technol. **32**, 3317–3323 (2014).

#322872 https://doi.org/10.1364/OE.26.012432
Journal © 2018 Received 9 Feb 2018; revised 26 Mar 2018; accepted 27 Mar 2018; published 1 May 2018

Optics EXPRESS

14. J. Jeganathan, A. Ghrayeb, and L. Szczecinski, "Spatial modulation: optimal detection and performance analysis," IEEE Commun. Lett. **12**, 545–547 (2008).
15. G. P. Agrawal, *Nonlinear fiber optics* (Academic, 2007).

1. Introduction

Due to the rapidly expanding mobile industry and the emerging Internet of Things (IoT), meeting the demands of seemless, low-latency communication requires the exploration of using new radio frequencies and employing more base-staions to improve the channel capacity and to reduce the Inter-Channel-Interference (ICI) [1]. Given the shortage of radio frequencies, the current cellular network is unable to meet the mobile subscribers' demand, hence there is an urgent need for more base-stations. As a benefit of the centralized processing capability of Radio over Fiber (RoF) solutions [2], technologies conceived for dense coverage at a low cost, such as the small-cell front-haul and cloud radio access network (C-RAN), where the base-station at the central office feeds radio access points (RAPs), tend to rely on RoF techniques to support the cellular network [3–6]. We previously proposed to centralize wireless beamforming and space-time-block-coding using RoF techniques to support wireless MIMO systems [2]. In this treatise, we conceive an all-optical Spatial Modulation (SM) scheme relying on optical single side-band modulation.

SM belongs to the family of Multiple-Input-Multiple-Output (MIMO) schemes, which aim for reducing both the complexity and the Inter-Channel Interference (ICI) imposed by multiple-antenna systems, where only a single RF-chain is required [7]. Additionally, SM is considered to be a strong candidate for next-generation communication systems [8–10]. To elaborate a little further, SM activates one out of multiple transmit antennas for conveying extra symbols [8, 11]. However, in order to select the activated antenna, switches are required for selecting the transmitting antenna, which adds complexity, where the number of switches increases linearly with the number of RAPs [10]. For example, a small-cell network with a cluster size of L RAPs requires L high speed switches. Actively powered switches are used by each RAP, increasing the power consumption upon increasing the number of RAPs.

Thus, in the context of C-RAN and small-cell front-hauls, which support both cost-effective management as well as site maintenace and network updates [4,5], our RoF technique is beneficial in terms of eliminating the actively powered switches as well as the power-thirsty high-precision digital-to-analog conversion (DAC) and analog-to-digital conversion (ADC) from the RAPs by centralizing the antenna selection processing. Furthermore, the passively pre-set optical filters in the RAPs of our design allow convenient antenna selection information detection. Thus, in order to integrate SM into the centralized processing aided RoF network, we propose to amalgamate SM with a RoF system for simplifying the transceiver design. In our design, the SM antenna selection is represented by the side-bands of an Optical Single Side-Band (OSSB) signal generated by a dual-drive Mach-Zehnder Modulator (MZM). More specifically, we index the OSSB location using the phase-shifting techniques proposed in [12, 13], realizing an optical processing aided low-cost SM encoding, where only a single RF chain is required to serve a single RAP. Thus, SM encoding takes place in a central office, while the RAPs are responsible for optical filtering, Optical-to-Electrical (O-E) conversion, electronic amplification and transmission. As a benefit, there is no need for agile switches at the wireless transmitter. Our contributions in this paper are summarised as follows:

1. We design an energy-efficient RoF network relying on twin-antenna SM encoding at the central office, where the SM switches are eliminated, hence significantly simplifying the transceiver design and reducing both the complexity as well as the power consumption of the RAPs of the conventional architecture relying on actively powered SM switches. This design can also be used in the context of C-RANs and small-cell front-hauls for facilitating

Optics EXPRESS

cost-effective management and site maintenance.

2. The sophisticated SM encoding philosophy is intrinsically integrated into our RoF design, where we view the optical side-band position as the antenna selection index, thus realising an all-optical central processing aided SM system architecture. The single-RF chain advantage of SM reduces the complexities of both the central office and of the RAPs.

3. We experimentally characterize the critical elements of our system by demonstrating a 2 Gbps RoF-aided Binary Phase Shift Keying (BPSK) SM system combined with convolutional coding, where we show that the SNR performance is less than 1 dB away from that of the system operating without the RoF.

4. Our design example employs 3 GHz radio carrier frequency. However, our proposed system design is scalable to any carrier frequency, where the radio carrier frequency is based on the drive frequency of the MZM.

The outline of the paper is as follows. We propose our system design based on our simulation model in Section 2, after which the experimental results are provided for verification in Section 3 followed by our conclusions in Section 4.

2. Proposed RoF-aided SM system

In this section, we introduce our RoF-aided twin-antenna SM system design and present our simulation-based performance analysis.

2.1. Conventional SM scheme

In the conventional SM scheme, the transmitted data is firstly split into two streams, as shown in Fig. 1, where the upper stream corresponds to the implicitly conveyed information used for antenna selection, while the lower stream to the classic modulated symbol transmission, namely Quaduature Amplitude Modualation/Phase Shift Keying (QAM/PSK). As shown in Fig. 1, the switch activating the specific antenna used for wireless transmission relies on the antenna selection information assigned to the upper stream of Fig. 1. For example, a twin-antenna SM scheme requires one-bit of information to control the switch-option, where a logical 1 can activate antenna 1 while a logical 0 activates antenna 2 corresponding to the lower side-band and upper side-band in our system to be elaborated on in the next section. Generally speaking, a classic N-bit information symbol can be conveyed over the lower stream of Fig. 1. At the receiver side, the classic symbols as well as the antenna selection symbols can be jointly interpreted by Maximum Likelihood (ML) detection [14].

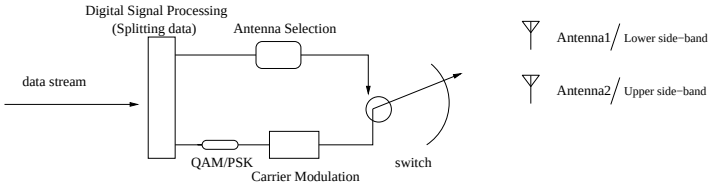

Fig. 1. Conventional twin-antenna SM scheme adapted to SB-switching.

Instead of implementing the SM encoding scheme at each RAP, which adds extra complexity constituted by the antenna-switches, we propose a RoF system, which optically encodes the SM symbols in a central office with the aid of centralized processing, where the actively powered switches are replaced by the passive optical components of the RAPs. As a benefit, we can

Optics EXPRESS

dispense with power-thirsty high-precision digital-to-analog conversion (DAC) and analog-to-digital conversion (ADC) in the RAPs. Note that the number of passive optical components required in the RAPs increase linearly with the number of RAPs, however, as a benefit of the low-power RAPs proposed, we conceived an energy-efficient and cost-efficient RoF-aided front-haul system. Next, we detail our RoF-aided system design and characterize it.

2.2. Proposed RoF-aided SM design

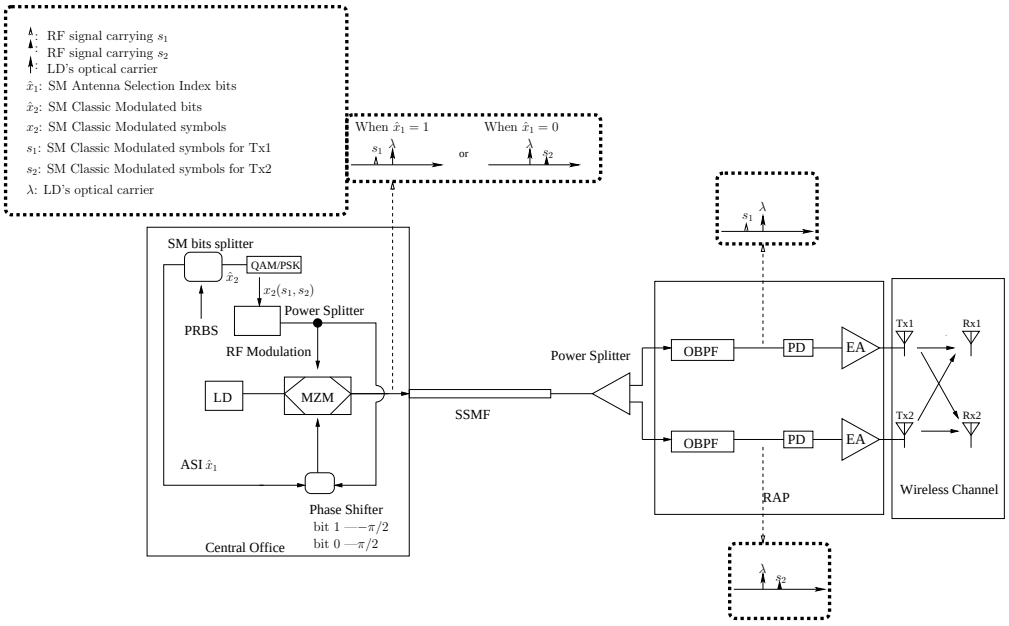

Fig. 2. System schematic of RoF-aided twin-antenna SM downlink system. PRBS: Pseudorandom Binary Sequence, ASI: Antenna Selection Information, DSP: Digital Signal Processing, LD: Laser Diode, RF: Radio Frequency, MZM: Mach-Zehnder Modulator, OBPF: Optical Band Pass Filter, PD: Photo Detector, EA: Electronic Amplfier, RAP: Radio Access Point, Tx: Transmitter, Rx: Receiver.

Let us now consider our RoF-aided twin-antenna SM system shown in Fig. 2, where we show both the RoF link and the wireless link. In our system, we externally modulate the Radio Frequency (RF) signal into the Optical Carrier (OC) generated by a Laser Diode (LD) using a dual-drive MZM, which can be set to operate in a specific Optical Single Side-Band (OSSB) mode during each symbol period. The OSSB signal can be generated by setting the phase difference of the RF signal in both arms of the MZM to $\pi/2$ or $-\pi/2$, where one of the first-order side-bands would be suppressed [12, 13]. Specifically, to centralize the SM encoding, phase-controlled side-band suppression is exploited. As discussed and experimentally verified in [12, 13], by imposing a phase-difference of $\pi/2$ or $-\pi/2$ between each arm of a dual-drive MZM, one of the first-order side-bands of the modulated optical signals will be suppressed. We exploit a dual-drive MZM to interpret specific side-band used as the antenna selection index of SM. As shown in Fig. 2, a phase-shifter is employed to change the phase-difference of the MZM's arms of Fig. 2 to either $-\pi/2$ or $\pi/2$.

In our design, as shown in Fig. 2, a pseudorandom binary sequence (PRBS) input is split into the SM antenna selection index bits $\hat{x}_1$ and the SM classic modulated bits $\hat{x}_2$, where $\hat{x}_1$ controls the phase shifter of Fig. 2 and $\hat{x}_2$ is mapped to the classic QAM/PSK symbols x_2. The symbols x_2 are then carried by a RF signal, which is power-split to both MZM arms and used as the drive

Optics EXPRESS

voltages of the dual-drive MZM of Fig. 2. Furthermore, the side-band selection process, which corresponds to the antenna selection in conventional wireless SM, is detailed in Fig. 3. As shown in Fig. 3, when the antenna selection bit 1 is transmitted, the phase-shift $-\pi/2$ is chosen, which maps the QAM/PSK-modulated RF signal to the lower side-band, while the antenna selection bit 0 encodes it to the upper side-band of the optical carrier generated by the LD of Fig. 2, which corresponds to a phase-shift of $\pi/2$.

Following the SM encoding and the transmission of the signal through a Standard Single Mode Fiber (SSMF), the optical signal is power-split and fed into two different lines, where the upper line retains the lower side-band and the bottom line obtains the upper side-band using an optical band pass filter (OBPF), as shown in Fig. 2. Then, the filtered optical signal of each line will be converted to the corresponding electronic signal and passed through Electronic Amplifiers (EAs) for amplification, where the symbols s_1 conveyed by the lower side-band are carried by an RF signal and feed the Transmitter (Tx) antenna 1 (Tx1), while the symbols s_2 conveyed by the upper side-band feed the Tx antenna 2 (Tx2). Subsequently, the SM symbols mapped to the RF signals are transmitted over the wireless channel without any signal processing in the RAPs of Fig. 2. Thus, our SM antenna selection information selects the antennas using our new side-band selection technique, while classic symbols are mapped to the corresponding side-band and converted to RF signals. To elaborate a little further, Fig. 4 shows the OSSB power spectral density (PSD) of the RoF-aided SM signal after each OBPF of the RAP of Fig. 2, where the left plot corresponds to the bit-1-selected lower side-band conveying information to Tx1 of Fig. 2, while the upper side-band shown in the right plot is the bit-0-selected signal conveying information to Tx2. The central frequency of 200 GHz shown in Fig. 4 is selected for the convenience of simulation, which is relative to 193.1 THz.

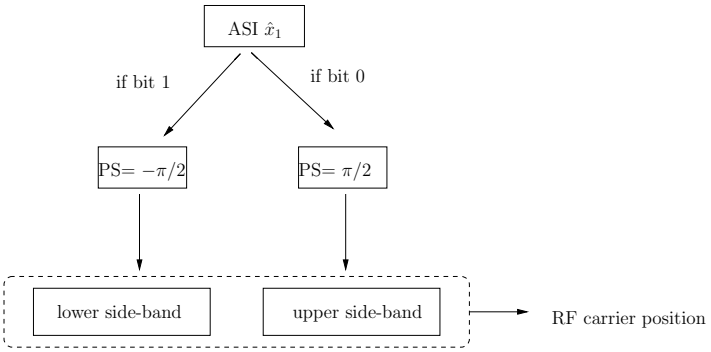

Fig. 3. Side-band Selection. ASI: Antenna Selection Information, PS: Phase Shift.

As a benefit, any electronic digital signal processing as well as SM encoding switches can be completely eliminated in the RAPs of Fig. 2. Furthermore, the OBPFs on each line of the RAPs of Fig. 2 are utilized to select the required side-band for each antenna. Through side-band filtering, the output of each branch in the RAP of Fig. 2 is passed to the corresponding antennas for SM transmission. Thus, the passively preset OBPFs of Fig. 2 are capable of replacing the function of actively powered switches, hence substantially reducing both the system complexity and the power consumption imposed on the RAPs.

2.3. Characterization performance

Prior to experimental verification, the proposed system was simulated using MATLAB. In our simulations, an RF frequency of 3 GHz was externally modulated by an optical carrier of 1550 nm. The Split-Step Fourier Method was used as our channel model [15].

Optics EXPRESS

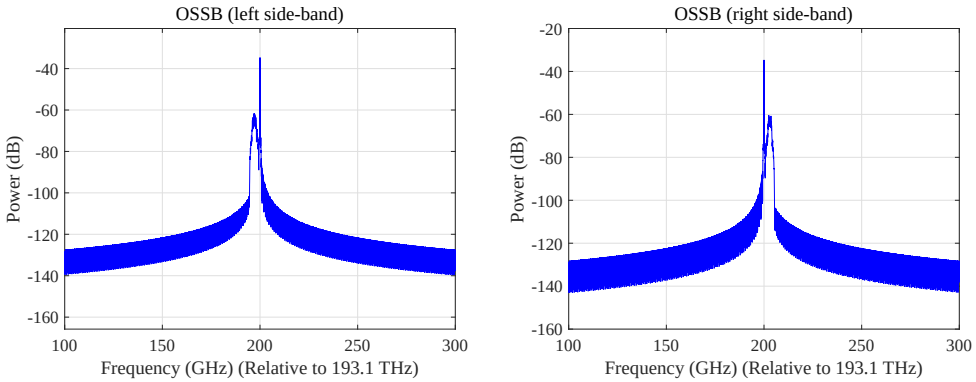

(a) Left Side-Band. (b) Right Side-Band.

Fig. 4. PSD of the OSSB for Side-Band Selection.

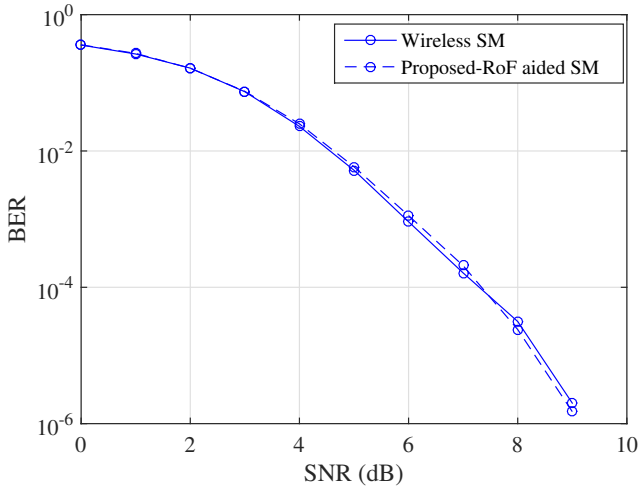

Fig. 5. Simulated BER performance of proposed RoF-aided twin-antenna SM system.

A convolutional code having a code rate of $1/2$, a constraint length of 7 and generator polynomials of (171,133) (in octal) was used. As shown in Fig. 2, the classic modulated bits are mapped to Binary Phase Shift Keying (BPSK) symbols. The classic modulated BPSK symbol is then mapped to the lower side-band of the LD's optical carrier of Fig. 2 when a logical one antenna-selection information is applied and vice versa. This is carried by controlling the phase shifter of Fig. 2 by $\pi/2$ or $-\pi/2$. Then, the SM encoded optical signal is transmitted over a 20 km SSMF, where a power splitter is imposed after the fiber transmission in order to extract the side-band information for mapping to the corresponding antennas. Afterwards, the preset OBPF, PD and EA filters the signal and converts the optical signal to 3 GHz RF signal. Thus, the RF signal carrying the SM symbols is transmitted from the two antennas. In the wireless link, we simulated a Rayleigh-fading channel and we employed maximum likelihood (ML) detection [14].

Figure 5 shows the Bit Error Ratio (BER) performance of a 2×2 SM scheme employing our RoF-aided design, which is compared to a 'wireless-only' SM scheme operating without the RoF link for the sake of showing the feasibility of intrinsically amalgamating SM with our proposed RoF system. The 'wireless-only' SM scheme represents the conventional SM scheme, when

Optics EXPRESS

only wireless transmission is considered and no RoF link is involved. The wireless channel used is a Rayleigh-fading channel. The Signal-to-Noise Ratio (SNR) indicated in Fig. 5 is the wireless SNR, where we show that our RoF-aided SM system has modest impact on the system's performance. Additionally, our 2×2 SM prototype scheme can be readily extended to an arbitrary number of receive antennas. Based on the analysis above, we will experimentally characterize our system and the experiment will be detailed in the next section.

Table 1. Experimental Parameters

Parameter	Value
Bit rate	2 Gbps (with convolutional code)
RF drive signal	3 GHz
LD center wavelength	1550.134 nm
Optical power before MZM modulation	9.35 dBm
MZM DC bias	2.68 V
Input power of Fiber	1.5 dBm
Fiber type	Standard Single Mode Fiber at 1550 nm
Fiber length	20 km
Modulation type	BPSK
OBPFs central wavelength	1550.174 nm and 1550.094 nm
OBPFs 3 dB bandwidth	0.114 nm
PD data bandwidth	10 Gbps
LPF cutoff frequency	3.9 GHz
Wireless Channel	Rayleigh-fading Channel
Wireless Detection	Maximum Likelihood Detection

3. Experimental setup

To further verify our proposed system, we have demonstrated our system design as shown in Fig. 6. The dual-drive MZM used is of 40 Gbps relying on the Model T.DEH1.5-40PD-ADC from SUMITOMO OSAKA CEMENT. A Standard Single Mode Fiber (SSMF) of 20 km is utilized. The input power of the fiber is 1.5 dBm.

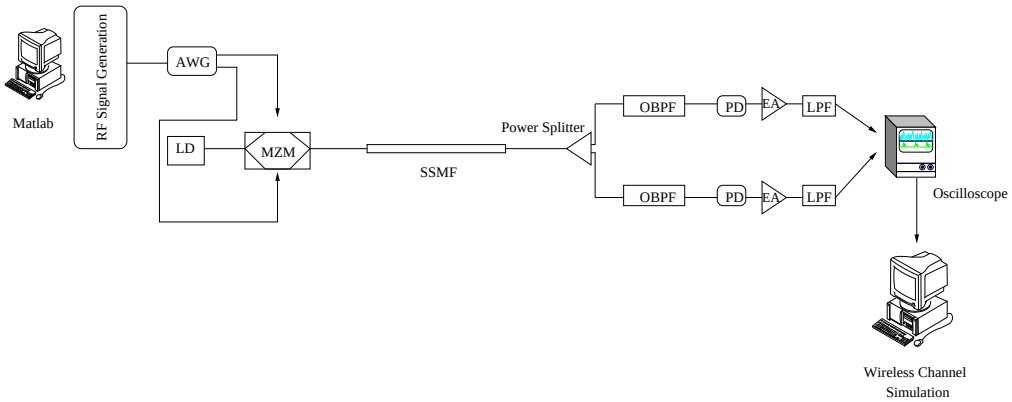

Fig. 6. Experimental Setup.

In our experiment, the RF signals are fed into the MZM of Fig. 6 for side-band selection, which are processed in MATLAB offline on a computer and then generated by an Arbitrary

Optics EXPRESS

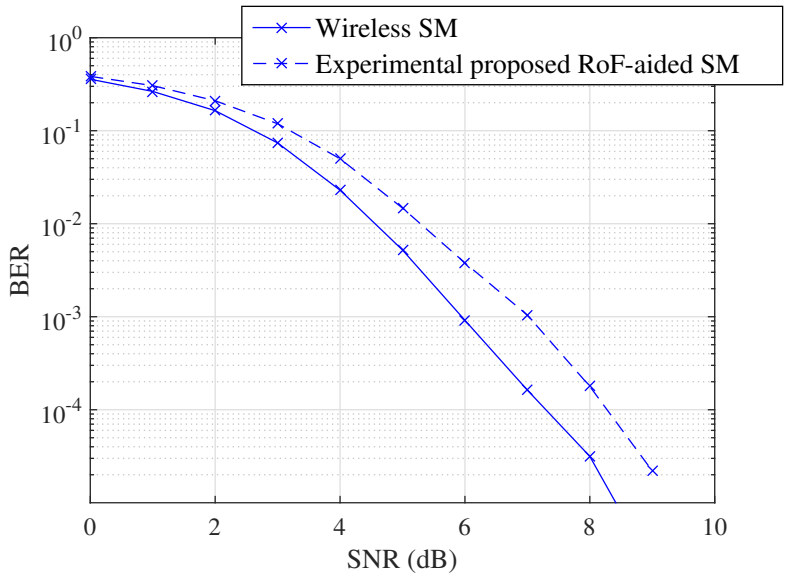

Fig. 7. Experimental demonstration BER of proposed RoF-aided twin-antenna SM BER performance.

Waveform Generator (AWG). Specifically, we generated a pair of BPSK-modulated RF carriers at 3 GHz in MATLAB. Then, one of the RF signals is phase shifted by $\pi/2$ or $-\pi/2$ according to the SM antenna selection bits $\hat{x_1}$, with both of the offline-processed signals being entered into an AWG operated at 12 GSamples/s to drive each arm of the dual-drive MZM for the sake of side-band selection. As a result, the signal driving the bottom arm of Fig. 6 is phase-shifted off-line in Matlab for SM encoding, thus ensuring that the phase-difference of the drive signal of each arm remains either $\pi/2$ or $-\pi/2$. After the side-band selection by MZM of Fig. 6, the signal is transmitted over a 20 km SSMF. At the fiber's receiver side, after OBPF, PD, EA and a Low Pass Filter (LPF), the signal of each branch of Fig. 6 is passed to an oscilloscope, where we visualize the output signal for a 2×2 SM MIMO analysis. The normalized signal of the oscilloscope is exploited as the wireless input signal simulated in MATLAB. Again, the wireless channel is simulated as a Rayleigh-fading channel and ML detection is used at the wireless receiver side. The stylized real-world implementation is portrayed in Fig. 2. In our experiment, we opted for implementing the critical components of our proposed design, while the associated large-scale wireless system and some of the electronic devices, such as the phase shifter of Fig. 2, were simulated in MATLAB. The parameters of this experiment are shown in Table 1 and the demonstration system is portrayed in Fig. 6.

As demonstrated in Table 1, a convolutional code having a code rate of 1/2, a constraint length of 7 and generator polynomials of (170,133) (in octal) is used in our system. To show the effect of our proposed system on the BER performance, we also plotted in Fig. 7 the 'wireless-only' SM BER curve as well as the experimental RoF-aided twin-antenna SM system BER, where we show that the experimental results exhibit about 1 dB degradation at BER of 10^{-4} compared to the simulation results of the 'wireless-only' SM without RoF as well as that with RoF of Fig. 5. This disparity is partially caused by the phase noise introduced by the optical components and by the frequency leakage of the OBPFs used. Nonetheless, given that only 1 dB degradation is observed at BER of 10^{-4}, we realized a RoF-aided twin-antenna SM system, dispensing with both digital processing and with actively powered SM switches in the RAP, resulting in an energy-efficient RoF-aided SM system.

Optics EXPRESS

4. Conclusion

In this paper, we designed an all-optical processing RoF-aided SM scheme. An experimental demonstration of the novel RoF-aided twin-antenna SM system has been proposed, simplifying transceiver design and reducing the power consumption of the conventional SM switches. SM encoding was implemented in the optical domain and our centralized RoF-aided SM encoding using MZM's side-band selection was analysed and verified by experiments. This design can be implemented by C-RAN as well as small-cell front-haul solutions. The experimental results show that our 2 Gbps system exhibits only marginally degraded BER performance compared to those operating without RoF while benefiting from centralized SM encoding and RAP switch removal.

Funding

H2020 European Research Council (Adavnced Fellow Grant).